Bulgarian Chemical Communications, Volume 49, Number 2, (pp. 320 – 330) 2017

Analytical and numerical study of the diffusion of chemically reactive species in an Eyring-Powell fluid over an oscillatory stretching surface

S.U. Khan[1*], N. Ali[2] , T. Hayat[3, 4]

[1]*Department of Mathematics, COMSATS Institute of Information Technology, Sahiwal 57000, Pakistan*
[2]*Department of Mathematics and Statistics, International Islamic University, Islamabad 44000, Pakistan*
[3]*Department of Mathematics, Quaid-i-Azam University 45320, Islamabad 44000, Pakistan*
[4]*Nonlinear Analysis and Applied Mathematics (NAAM) Research Group, Department of Mathematics, Faculty of Science, King Abdulaziz University, Jeddah 21598, Saudi Arabia*

Received October 3, 2015; Revised July 14, 2016

This study deals with the unsteady flow of an Eyring-Powell fluid induced by an oscillatory stretching surface in presence of chemical reaction. The elastic sheet is stretched periodically back and forth in its own plane. The equations governing the flow are derived employing fundamental law of mass, momentum and diffusion. The independent variables in the governing equations are reduced by using dimensionless variables which are solved by using two different techniques, namely, homotopy analysis method and an implicit finite difference scheme. Solutions obtained by both methods are compared and found in excellent agreement. The physical variables such as longitudinal velocity component and mass concentration are examined in detail for various values of the parameters of interest.

Keywords: Eyring-Powell fluid, chemical effects, oscillatory stretching sheet, Homotopy analysis method, finite difference scheme.

INTRODUCTION

The study of convective flow under the influence of magnetic field and chemical reaction has practical applications in many areas of science and engineering. This phenomenon plays a vital role in chemical industry, petroleum industry, cooling of nuclear reactors, packed-bed catalytic reactors, etc. In view of all these applications many researchers studied the effects of chemical reaction on the flow of different fluids. The specialized literature on this topic is discussed in the following paragraphs. Chambre and Young [1] discussed the diffusion of a chemically reactive species in a laminar boundary layer flow over a flat plate. Andersson et al. [2] studied the laminar boundary layer flow induced by a stretching sheet in the presence of chemical reaction effects. Takhar et al. [3] discussed the diffusion of chemically reactive species in a second-order fluid over a stretching sheet. Akyildiz et al. [4] studied the diffusion of chemically reactive species in a second-grade fluid over a porous stretching surface. Hayat and Abbas [5] used homotopy analysis to analyze the effects of chemical reaction in a Maxwell fluid. In another paper, Hayat et al. [6] examined the effects of mass transfer in a unsteady flow of Maxwell fluid over a stretching sheet. The effect of chemical reaction and variable viscosity with heat and mass transfer for a Hiemenz flow through a Darcian porous medium was investigated by Seddeek et al. [7]. Aziz [8] used a numerical technique to discuss the effects of chemical reaction and heat mass transfer in a viscous fluid.

Ferdows and Qasem [9] investigated the effects of the order of chemical reaction on a boundary layer flow with heat mass transfer over a linearly stretching surface. Krishnendu [10] discussed the effects of mass transfer in presence of chemical reaction over a porous flat plate. Mukhopadhyay and Bhattacharyya [11] used a shooting method to analyze the first-order constructive/destructive chemical reaction in a flow of Maxwell fluid over a stretching sheet. The chemically reactive hydromagnetic flow of a second-grade fluid in a semi-porous channel was discussed by Abbas et al. [12]. Apart of these, some recent attempts regarding flows of different fluids in presence of chemically reactive species can be found in refs. [13-17].

Motivated by the studies mentioned above, the aim of this paper is to analyze the unsteady flow and mass transfer of chemically reactive species. The rheological behavior of the fluid is captured by the constitutive equation of the Eyring-Powell model. This model has already been used by several authors to discuss non-Newtonian flows [18-21]. Unlike typical studies, the stretching sheet is assumed to be oscillatory. The idea of flow over an oscillatory stretching sheet was introduced by Wang [22]. The work of Wang [22] was extended by few authors including Siddapa et al. [23], Abbas et al. [24, 25], Zheng et al. [26] and Ali et al. [27].

* To whom all correspondence should be sent:
E-mail: sk_iiu@yahoo.com

© 2017 Bulgarian Academy of Sciences, Union of Chemists in Bulgaria

The proposed study extends the analysis of Wang [22] by considering an Eyring-Powell fluid model in the presence of chemically reactive species. The solution of the governing problem is obtained by a homotopy analysis method (HAM) and a finite difference scheme. A comparison of both solutions is made. Based on the numerical solution a parametric study is carried out to quantify the effects of various emerging parameters on the flow and concentration characteristics inside the boundary layer.

FLOW ANALYSIS

Let us consider an unsteady, two-dimensional and magnetohydrodynamic (MHD) flow of an incompressible Eyring-Powell fluid past over an oscillatory stretching sheet coinciding with plane $\bar{y}=0$ (see Fig. 1).

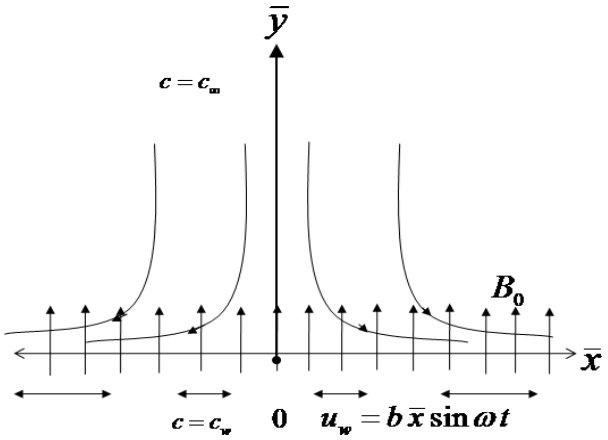

Fig. 1. Geometry of the problem.

The elastic sheet is periodically stretched back and forth with a velocity $u_w = b\bar{x}\sin\omega t$ ($\bar{x}$ is the coordinate along the sheet, b is the maximum stretching rate and ω represents the frequency). A magnetic field of magnitude B_0 is applied in the direction perpendicular to the sheet. Let c_w denotes the concentration at the surface while the concentration far away from the surface is c_∞. The continuity, momentum and concentration equations for an Eyring-Powell fluid can be expressed as [21]

$$\frac{\partial u}{\partial \bar{x}}+\frac{\partial v}{\partial \bar{y}}=0, \tag{1}$$

$$\frac{\partial u}{\partial t}+u\frac{\partial u}{\partial \bar{x}}+v\frac{\partial u}{\partial \bar{y}}=\left(\nu+\frac{1}{\rho\beta^* C}\right)\frac{\partial^2 u}{\partial \bar{y}^2} -\frac{1}{2\rho\beta^* C^3}\left[\left(\frac{\partial u}{\partial \bar{y}}\right)^2\frac{\partial^2 u}{\partial \bar{y}^2}\right]-\frac{\sigma B_0^2}{\rho}u, \tag{2}$$

$$\frac{\partial c}{\partial t}+u\frac{\partial c}{\partial \bar{x}}+v\frac{\partial c}{\partial \bar{y}}= D\frac{\partial^2 c}{\partial \bar{y}^2}-k\left(c-c_\infty\right), \tag{3}$$

where u and v are velocity components along $\bar{x}$ and $\bar{y}$ directions, respectively, ν represents the kinematic viscosity, ρ is the density, β^* and C denote the material parameters of the Eyring-Powell model, c is the concentration field, D is the concentration expansion coefficient, k is the chemical reaction rate.

Eqs. (1)-(3) are subjected to the conditions

$$u=u_\omega=b\bar{x}\sin\omega t,\quad v=0,\ c=c_w \text{ at } \bar{y}=0,\quad t>0, \tag{4}$$

$$u\to 0,\quad c\to c_\infty \qquad \text{at} \qquad \bar{y}\to\infty, \tag{5}$$

Let us introduce appropriate variables [22, 24]

$$y=\sqrt{\frac{b}{\nu}}\bar{y},\qquad \tau=t\omega, \tag{6}$$

$$u=b\bar{x}f_y\left(y,\tau\right),\quad v=-\sqrt{\nu b}\,f\left(y,\tau\right),$$

$$\phi\left(y,\tau\right)=\frac{c-c_\infty}{c_w-c_\infty}. \tag{7}$$

Utlizing Eqs. (6) and (7), Eq.(1) is identically satisfied and Eqs. (2) and (3) become

$$\left(1+K\right)f_{yyy}-Sf_{y\tau}-f_y^2+ff_{yy}-M^2f_y-\lambda Kf_{yy}^2f_{yyy}=0, \tag{8}$$

$$\phi_{yy}+Sc\left(f\phi_y-S\phi_\tau\right)-Sc\beta\phi=0, \tag{9}$$

with boundary conditions

$$f_y\left(0,\tau\right)=\sin\tau,\quad f\left(0,\tau\right)=0,\quad \phi\left(0,\tau\right)=1, \tag{10}$$

$$f_y\left(\infty,\tau\right)=0,\qquad \phi\left(\infty,\tau\right)=0. \tag{11}$$

In the above equations $K=1/\mu\beta^*C$ and $\lambda=\bar{x}^2b^3/2\nu C^2$ are dimensionless material fluid parameters, $S\equiv\omega/b$ is the ratio of the oscillation frequency of the sheet to its stretching rate, $M=\sqrt{\sigma B_0^2/\rho b}$ is the Hartmann number, $Sc=\upsilon/D$ is the Schmidt number and $\beta=k/b$ denotes the chemical reaction parameter. According to Javed et al. [18], Eq. (2) is subject to the constraint $\lambda K<<1$.

The skin-friction coefficient C_f is defined as

$$C_f = \frac{\tau_w}{\rho u_w^2}, \tag{12}$$

where τ_w denotes the shear stress at the wall. In view of (6) and (7), Eq. (12) takes the following form [19]

$$\mathrm{Re}_x^{1/2} C_f = \left[(1+K) f_{yy} - \frac{K}{3} \beta f_{yy}^{\ 3} \right]_{y=0}, \tag{13}$$

where $\mathrm{Re}_x = u_w \bar{x} / \nu$ is the local Reynold number.

HOMOTOPY ANALYSIS METHOD

Homotopy analysis method is one of the powerfull analytic approaches to solve nonlinear partial and ordinary differential equations. This method was proposed by Liao [28] and then used by many authors for solution of different nonlinear problems [29-34]. Now we briefly describe the application of this method to the boundary value problem developed in the previous section. The boundary conditions lead to the following initial guesses for $f(y,\tau)$ and $\phi(y)$

$$\begin{aligned} f_0(y,\tau) &= \sin\tau\left(1-\exp(-y)\right), \\ \phi_0(y) &= \exp(-y). \end{aligned} \tag{14}$$

Introducing linear operators

$$\pounds_f(f) = \frac{\partial^3 f}{\partial y^3} - \frac{\partial f}{\partial y}, \ \pounds_\phi(f) = \frac{\partial^2 f}{\partial y^2} - f, \tag{15}$$

satisfying

$$\pounds_f\left[C_1 + C_2\exp(-y) + C_3\exp(y)\right] = 0, \tag{16}$$

$$\pounds_\phi\left[C_4\exp(-y) + C_5\exp(y)\right] = 0, \tag{17}$$

where C_i $(i = 1,2,...5)$ are constants. The zero[th]-order deformation problems defined

$$(1-p)\pounds_f\left[\hat{f}(y,\tau;p) - f_0(y,\tau)\right] = p\hbar_f N_f\left[\hat{f}(y,\tau;p)\right], \tag{18}$$

$$(1-p)\pounds_\phi\left[\hat{\phi}(y,\tau;p) - \hat{\phi}_0(y,\tau)\right] = p\hbar_\phi N_\phi\left[\hat{f}(y,\tau;p), \hat{\phi}(y,\tau;p)\right], \tag{19}$$

$$\hat{f}(0,\tau;p) = 0, \left.\frac{\partial \hat{f}(y,\tau;p)}{\partial y}\right|_{y=0} = \sin\tau, \left.\frac{\partial \hat{f}(y,\tau;p)}{\partial y}\right|_{y\to\infty} = 0. \tag{20}$$

$$\hat{\phi}(0,\tau;p) = 1, \quad \hat{\phi}(\infty,\tau;p) = 0, \tag{21}$$

where $p \in [0,1]$ is an embedding parameter. The associated nonlinear operators N_f and N_ϕ are

$$\begin{aligned} N_f\left[\hat{f}(y,\tau;p)\right] &= (1+K)\frac{\partial^3 \hat{f}(y,\tau;p)}{\partial y^3} - S\frac{\partial^2 \hat{f}(y,\tau;p)}{\partial y \partial \tau} - \\ & M^2\frac{\partial \hat{f}(y,\tau;p)}{\partial y} - \left(\frac{\partial \hat{f}(y,\tau;p)}{\partial y}\right)^2 + \hat{f}(y,\tau;p)\left(\frac{\partial^2 \hat{f}(y,\tau;p)}{\partial y^2}\right) \\ & -\lambda K\left(\frac{\partial^2 \hat{f}(y,\tau;p)}{\partial y^2}\right)^2\left(\frac{\partial^3 \hat{f}(y,\tau;p)}{\partial y^3}\right), \end{aligned} \tag{22}$$

$$\begin{aligned} N_\phi\left[\hat{\phi}(y,\tau;p), \hat{f}(y,\tau;p)\right] &= \frac{\partial^2 \hat{\phi}(y,\tau;p)}{\partial y^2} + \\ & Sc\left(\hat{f}(y,\tau;p)\frac{\partial \hat{\phi}(y,\tau;p)}{\partial y} - S\frac{\partial \hat{\phi}(y,\tau;p)}{\partial \tau}\right) - \beta Sc\phi \end{aligned} \tag{23}$$

The zero[th]-order deformation problems defined above have the following solutions corresponding to $p = 0$ and $p = 1$

$$\hat{f}(y,\tau;0) = f_0(y,\tau), \ \hat{f}(y,\tau;1) = f(y,\tau), \tag{24}$$

$$\hat{\phi}(y,\tau;0) = \phi_0(y,\tau), \hat{\phi}(y,\tau;1) = \phi(y,\tau). \tag{25}$$

Using Taylor's series expansion, we can write

$$\begin{aligned} \hat{f}(y,\tau;p) &= f_0(y,\tau) + \sum_{m=1}^{\infty} f_m(y,\tau)\, p^m, \\ f_m(y,\tau) &= \frac{1}{m!}\left.\frac{\partial^m \hat{f}(y,\tau;p)}{\partial p^m}\right|_{p=0}, \end{aligned} \tag{26}$$

$$\begin{aligned} \hat{\phi}(y,\tau;p) &= \phi_0(y,\tau) + \sum_{m=1}^{\infty} \phi_m(y,\tau)\, p^m, \\ \phi_m(y,\tau) &= \frac{1}{m!}\left.\frac{\partial^m \hat{\phi}(y,\tau;p)}{\partial p^m}\right|_{p=0}. \end{aligned} \tag{27}$$

The convergence of the above series solution depends upon $\hbar_f$ and $\hbar_\phi$. We assume that $\hbar_f$ and $\hbar_\phi$ are selected so that Eqs. (25) to (26) converges at $p = 1$. Therefore

$$f(y,\tau) = f_0(y,\tau) + \sum_{m=1}^{\infty} f_m(y,\tau), \tag{28}$$

$$\phi(y,\tau) = \phi_0(y,\tau) + \sum_{m=1}^{\infty} \phi_m(y,\tau), \tag{29}$$

The m^{th}-order of the deformation problem is

$$\pounds_f\left[f_m(y,\tau)-\chi_m f_{m-1}(y,\tau)\right]=h_f R_m^f(y,\tau), \quad (30)$$

$$\pounds_\phi\left[\phi_m(y,\tau)-\chi_m \phi_{m-1}(y,\tau)\right]=h_\phi R_m^\phi(y,\tau), \quad (31)$$

$$f_m(0,\tau)=0,\ \frac{\partial f_m(0,\tau)}{\partial y}=0,\ \frac{\partial f_m(\infty,\tau)}{\partial y}=0, \quad (32)$$

$$\phi_m(0,\tau)=\phi_m(\infty,\tau)=0, \quad (33)$$

$$R_m^f(y,\tau)=(1+K)\frac{\partial^3 f_{m-1}}{\partial y^3}-S\frac{\partial^2 f_{m-1}}{\partial y\partial\tau}-M^2\frac{\partial f_{m-1}}{\partial y}+\sum_{k=0}^{m-1}\left(\begin{array}{l} f_{m-1-k}\dfrac{\partial^2 f_k}{\partial y^2}-\dfrac{\partial f_{m-1-k}}{\partial y}\dfrac{\partial f_k}{\partial y}- \\ \lambda K\dfrac{\partial^2 f_{m-1-k}}{\partial y^2}\displaystyle\sum_{l=0}^{k}\dfrac{\partial^2 f_{k-1`}}{\partial y^2}\dfrac{\partial^3 f_{1`}}{\partial y^3}\end{array}\right), \quad (34)$$

$$R_m^\phi(y,\tau)=\frac{\partial^2\phi_{m-1}}{\partial y^2}-S(Sc)\frac{\partial\phi_{m-1}}{\partial\tau}-\beta Sc\phi_{m-1}+Sc\sum_{k=0}^{m-1}\left(f_{m-1-k}\frac{\partial\phi_k}{\partial y}\right). \quad (35)$$

$$\chi_m=\begin{cases}0, & m\le 1,\\ 1, & m>1.\end{cases} \quad (36)$$

The general solution at m^{th}-order can be expressed as

$$f_m(y,\tau)=f_m^*(y,\tau)+C_1+C_2\exp(-y)+C_3\exp(y), \quad (37)$$

$$\phi_m(y,\tau)=\phi_m^*(y,\tau)+C_4\exp(-y)+C_5\exp(y). \quad (38)$$

where $f_m^*(y,\tau)$ and $\phi_m^*(y,\tau)$ indicate the particular solutions. The constants C_i *(i = 1,2…,5)* using conditions (20) and (21) get values

$$C_3=C_5=0,\ C_2=\frac{\partial f_m^*(0,\tau)}{\partial y},\quad C_1=-C_2-f_m^*(0,\tau),\quad C_4=-\phi_m^*(0,\tau). \quad (39)$$

DIRECT NUMERICAL SOLUTION OF THE PROBLEM

The system of nonlinear partial differential equations (8)–(9) with the boundary conditions (10) and (11) are solved numerically using a finite difference scheme with Fortran software. We use coordinate transformation $\eta=1/(y+1)$ to transform the semi-infinite physical domain $y\in[0,\infty)$ to finite calculation domain $\eta\in[0,1]$, i.e.:

$$y=\frac{1}{\eta}-1,\quad \frac{\partial}{\partial y}=-\eta^2\frac{\partial}{\partial\eta},$$

$$\frac{\partial^2}{\partial y^2}=\eta^4\frac{\partial^2}{\partial\eta^2}+2\eta^3\frac{\partial}{\partial\eta},\quad \frac{\partial^2}{\partial y\partial\tau}=-\eta^2\frac{\partial^2}{\partial\eta\partial\tau},$$

$$\frac{\partial^3}{\partial y^3}=-\eta^6\frac{\partial^3}{\partial\eta^3}-6\eta^5\frac{\partial^2}{\partial\eta^2}-6\eta^4\frac{\partial}{\partial\eta}.$$

Using the above transformations in Eqs. (8) and (9)

$$S\frac{\partial^2 f}{\partial\eta\partial\tau}=\eta^2\left(\frac{\partial f}{\partial\eta}\right)^2+\left[6(1+K)\eta^2-2\eta f\right]\left(\frac{\partial f}{\partial\eta}\right)+\left[6(1+K)\eta^3-\eta^2 f\right]\left(\frac{\partial^2 f}{\partial\eta^2}\right)+(1+K)\eta^4\left(\frac{\partial^3 f}{\partial\eta^3}\right)$$
$$-M^2\left(\frac{\partial f}{\partial\eta}\right)-\lambda K\eta^{12}\left(\frac{\partial^2 f}{\partial\eta^2}\right)^2\left(\frac{\partial^3 f}{\partial\eta^3}\right)-$$
$$6\lambda K\eta^{11}\left(\frac{\partial^2 f}{\partial\eta^2}\right)^3-6\lambda K\eta^{10}\left(\frac{\partial f}{\partial\eta}\right)\left(\frac{\partial^2 f}{\partial\eta^2}\right)^2$$
$$-4\lambda K\eta^{10}\left(\frac{\partial f}{\partial\eta}\right)^2\left(\frac{\partial^3 f}{\partial\eta^3}\right)-$$
$$24\lambda K\eta^9\left(\frac{\partial f}{\partial\eta}\right)^2\left(\frac{\partial^2 f}{\partial\eta^2}\right)-24\lambda K\eta^8\left(\frac{\partial f}{\partial\eta}\right)^3$$
$$-4\lambda K\eta^{11}\left(\frac{\partial f}{\partial\eta}\right)\left(\frac{\partial^2 f}{\partial\eta^2}\right)\left(\frac{\partial^3 f}{\partial\eta^3}\right)-$$
$$24\lambda K\eta^{10}\left(\frac{\partial f}{\partial\eta}\right)\left(\frac{\partial^2 f}{\partial\eta^2}\right)^2-24\lambda K\eta^9\left(\frac{\partial f}{\partial\eta}\right)^2\left(\frac{\partial^2 f}{\partial\eta^2}\right) \quad (40)$$

$$\eta^4\frac{\partial^2\phi}{\partial\eta^2}+2\eta^3\frac{\partial\phi}{\partial\eta}-Sc\left(f\eta^2\frac{\partial\phi}{\partial\eta}+S\frac{\partial\phi}{\partial\tau}\right)-\beta Sc\phi=0, \quad (41)$$

$$f_\eta=0,\quad \phi=0 \quad \text{at} \quad \eta=0, \quad (42)$$

$$f=0,\quad f_\eta=-\sin\tau,\quad \phi=1 \ \text{at}\ \eta=1, \quad (43)$$

In the second step, we discretize Eqs. (18) and (19) for L equally spaced points $\eta=(\eta_0,\eta_1,\eta_2,...\eta_{L+1})\in[0,1]$ with a step size of $\Delta\eta=1/(L+1)$ at time instants $\tau=(\tau^1,\tau^2,...)$, where $\tau^i=\tau^1+i\Delta\tau$. The numerical values of $(f_1^n, f_2^n,..., f_L^n)$ and $(\phi_1^n, \phi_2^n, ..., \phi_L^n)$ are sought at these points at each time level provided that the boundary conditions at $\eta=\eta_0=0$ and $\eta=\eta_{L+1}=1$ are known. The initial conditions for velocity field are:

$$f(\eta,\tau=0)=0 \quad \text{and} \quad \phi(\eta,\tau=0)=0. \quad (44)$$

We construct the semi-implicit time difference scheme for f and ϕ as follows:

$$S\frac{1}{\Delta\tau}\left(\frac{\partial f^{(n+1)}}{\partial\eta}-\frac{\partial f^{(n)}}{\partial\eta}\right)=\eta^2\left(\frac{\partial f^{(n)}}{\partial\eta}\right)^2+$$
$$\left[6(1+K)\eta^2\right]\left(\frac{\partial f^{(n+1)}}{\partial\eta}\right)-2\eta f^{(n)}\left(\frac{\partial f^{(n)}}{\partial\eta}\right)+$$
$$6(1+K)\eta^3\left(\frac{\partial^2 f^{(n+1)}}{\partial\eta^2}\right)-2\eta f^{(n)}\left(\frac{\partial f^{(n)}}{\partial\eta}\right)-$$
$$\eta^2 f^{(n)}\left(\frac{\partial^2 f^{(n)}}{\partial\eta^2}\right)+(1+K)\eta^4\left(\frac{\partial^3 f^{(n+1)}}{\partial\eta^3}\right)-$$
$$M^2\left(\frac{\partial f^{(n+1)}}{\partial\eta}\right)-\lambda K\eta^{12}\left(\frac{\partial^2 f^{(n)}}{\partial\eta^2}\right)^2\left(\frac{\partial^3 f^{(n)}}{\partial\eta^3}\right)-$$
$$6\lambda K\eta^{11}\left(\frac{\partial^2 f^{(n)}}{\partial\eta^2}\right)^3-6\lambda K\eta^{10}\left(\frac{\partial f^{(n)}}{\partial\eta}\right)\left(\frac{\partial^2 f^{(n)}}{\partial\eta^2}\right)^2-$$
$$4\lambda K\eta^{10}\left(\frac{\partial f^{(n)}}{\partial\eta}\right)^2\left(\frac{\partial^3 f^{(n)}}{\partial\eta^3}\right)-$$
$$24\lambda K\eta^9\left(\frac{\partial f^{(n)}}{\partial\eta}\right)^2\left(\frac{\partial^2 f^{(n)}}{\partial\eta^2}\right)-24\lambda K\eta^8\left(\frac{\partial f^{(n)}}{\partial\eta}\right)^3-$$
$$4\lambda K\eta^{11}\left(\frac{\partial f^{(n)}}{\partial\eta}\right)\left(\frac{\partial^2 f^{(n)}}{\partial\eta^2}\right)\left(\frac{\partial^3 f^{(n)}}{\partial\eta^3}\right)- \quad (45)$$
$$24\lambda K\eta^{10}\left(\frac{\partial f^{(n)}}{\partial\eta}\right)\left(\frac{\partial^2 f^{(n)}}{\partial\eta^2}\right)^2-$$
$$24\lambda K\eta^9\left(\frac{\partial f^{(n)}}{\partial\eta}\right)^2\left(\frac{\partial^2 f^{(n)}}{\partial\eta^2}\right),$$

$$S(Sc)\frac{\left(\phi^{(n+1)}-\phi^{(n)}\right)}{\Delta\tau}=\left(\eta^4\frac{\partial^2\phi^{(n+1)}}{\partial\eta^2}+2\eta^3\frac{\partial\phi^{(n+1)}}{\partial\eta}\right)- \quad (46)$$
$$Scf^{(n)}\eta^2\frac{\partial\phi^{(n+1)}}{\partial\eta}-Sc\beta\phi.$$

The advantage of the scheme is that only linear equations for each new time step $(n+1)$ are to be solved. Two systems of linear equations for $f_i^{(n+1)}$ and $\phi_i^{(n+1)}$ at the time step $(n+1)$ can be solved by using Guassian elimination.

CONVERGENCE OF HAM SOLUTION AND ITS COMPARISON WITH A NUMERICAL SOLUTION

The convergence of HAM solution depends upon the suitable choice of auxiliary parameters $\hbar_f$ and $\hbar_\phi$. The *h*-curves are plotted in Fig. 2(a-b) to show the convergence region of the HAM solution for a particular set of involved parameters. From these figures it is clear that for this choice of parameter value a convergent solution can be obtained when $-1.4\leq\hbar_f<0$ and $-2\leq\hbar_\phi<0$.

To check the accuracy of HAM solution, the numerical values of $f''(0,\tau)$ at different order of approximations are shown in Table 1. The convergent values of $f''(0,\tau)$ can be obtained by increasing order of approximation. Figs. 3 and 4 show the comparison of HAM solution with a numerical solution at two different orders of approximation. An excellent agreement between HAM solution and numerical solution can be achieved at 15th order of approximation.

Table 1. The convergence of the HAM solution of $f''(0,\tau)$ for different order of approximation with $S=0.1$, $M=1.2$, $K=0.5$, $\lambda=0.4$ and $\tau=0$, $\tau=0.5\pi$ and $\tau=1.5\pi$, respectively.

Order of approximation	$\tau=0$	$\tau=0.5\pi$	$\tau=1.5\pi$
1	-0.02500	-1.26000	0.66400
3	-0.03363	-1.33995	0.563498
10	-0.03475	-1.36026	0.55218
12	-0.03475	-1.36048	0.55210
15	-0.03476	-1.36050	0.55210
25	-0.03476	-1.36050	0.55210
30	-0.03476	-1.36050	0.55210

RESULTS AND DISCUSSION

In this section graphical results obtained *via* a finite difference method are displayed in order to examine the effects of involved parameter on velocity component f' and concentration field ϕ. Fig. 5(a-c) demonstrates the effects of the relative amplitude of frequency to the stretching rate S, fluid parameters λ and Hartmann number M on the evolution series of the velocity component f' at a fixed distance $y = 0.25$ from the sheet, respectively. Fig. 5(a) shows that the amplitude of the flow motion at this location decreases by increasing S. However, this decrease is marginal and it is anticipated that such a trend is prevalent even for larger values of S. Fig. 5(b) depicts that the amplitude of the flow increases by increasing fluid parameter λ. This increase in the amplitude of flow motion is attributable to the increased effective viscosity induced by larger values of λ. The influence of Hartmann number M on time evolution of the velocity component f' is shown in Fig. 5(c). The figure reveals that the amplitude of the velocity component f' decreases by increasing Hartmann number.

The velocity profile f' for various values of S at four different distances $\tau = 8.5\pi$, $\tau = 9\pi$, $\tau = 9.5\pi$ and $\tau = 10\pi$ are shown in Fig. 6(a-d). Fig. 6(a) shows that at time instant $\tau = 8.5\pi$ the velocity decreases by increasing S. The back flow occurs near the surface where f' gets negative. The effects of S at time interval $\tau = 9\pi$ are depicted in Fig. 6(b). The velocity f' at this time instant oscillates near the surface and finally approaches zero. The amplitude of oscillation is found to increase with an increase in S. Fig. 6(c) elucidates that at time instant $\tau = 9.5\pi$, the velocity f' gets the value -1 at the wall and becomes zero far away from the surface without performing oscillation. A decrease in the amplitude of velocity is observed at this time instant. Fig. 6(d) reveals that at time instant $\tau = 10\pi$, the velocity f' is zero both at the surface and far away from the surface. It is also observed that at this time the amplitude of back flow increases by increasing S.

Fig. 7(a) shows the variation of f' for different values of λ at $\tau = 8.5\pi$. Here it is observed that the velocity approaches from 1 at the surface to zero far away from the surface. The occurrence of back flow near the surface is also observed at this time instant that is found to increase by increasing λ. Fig. 7(b) indicates that at this time instant $\tau = 9\pi$, the velocity oscillates near the surface before approaching zero far away from the surface. Moreover, the amplitude of the back flow is found to increase with λ. The variation of f' with λ at time instant $\tau = 9.5\pi$ is shown in Fig. 7(c). Here, the magnitude of velocity decreases by increasing λ. Occurrence of back flow at $\tau = 10\pi$ with its strengthening for larger values of λ is observed in Fig. 7(d).

Fig. 8(a-d) illustrates the effects of Sc, β, λ and S on the concentration profile ϕ. Fig. 8(a) is plotted to observe the effects of Smith number Sc on the concentration profile ϕ. From this figure we observe that mass concentration decreases for large values of Sc. Moreover, it is also seen from this figure that the concentration boundary layer thickness decreases by increasing Schmidt number Sc. These effects may be attributable to the increase in the rate of solute transfer from the surface by increasing the Schmidt number. The effect of chemical reaction parameter β on concentration is shown in Fig. 8(b). Here, we again observe that the mass concentration decreases by increasing β. Fig. 8(c) illustrates the effects of fluid parameter λ on the concentration profile ϕ. From this figure it is clear that the concentration increases by increasing fluid parameter λ. Fig. 8(d) shows opposite effects, i.e. mass concentration decreases by increasing the relative amplitude of frequency to the stretching rate parameter S. Fig. 9(a-d) describes the effects of relative amplitude of frequency to the stretching rate S, Hartmann number M and fluid parameters K and λ on the time-series of shear stress at the wall for the first five periods $\tau \in [0, 10\pi]$. Fig. 9(a) shows the influence of the relative amplitude of frequency to the stretching rate S on the skin-friction coefficient $\mathrm{Re}_x^{1/2} C_f$ by keeping other parameters fixed. It is clear from this figure that the amplitude of oscillation of the skin-friction coefficient increases by increasing the relative amplitude of frequency to the stretching rate S. From Figure 9(b) it is clear that the skin friction coefficient oscillates with time and the amplitude of oscillation increases for large values of Hartmann M. The effects of fluid parameter λ and K are illustrated in Figs. 9(c) and (d), respectively. These figures show an opposite trend, i.e. the skin friction coefficient $\mathrm{Re}_x^{1/2} C_f$ decreases monotonically by increasing these fluid parameters.

CONCLUSIONS

In the present study, we have investigated the mass transfer in a unsteady flow of an Eyring-Powell fluid model over an oscillatory stretching sheet. The non-similar solution of the governing nonlinear partial differential equations is obtained analytically by a homotopy analysis method and numerically by a finite difference scheme. The flow and mass transfer characteristics are explained graphically for the several values of the involved parameters. The main findings can be summarized as:

- The convergence of the HAM solution is largely dependent on the choice of auxiliary parameters and the order of approximation.
- The amplitude of the flow velocity at a fixed distance from the sheet decreases with increasing ratio of oscillating frequency to stretching rate S and Hartmann number M while a converse Eyring-Powell fluid parameter λ trend is computed with increasing λ.
- The concentration profile increases for large values of Eyring-Powell fluid parameter λ while it decreases for large values of Schmidt number Sc, ratio of oscillating frequency to stretching rate S and chemical reaction parameter β.
- The concentration boundary layer thickness decreases with increasing Schmidt number Sc, ratio of oscillating frequency to stretching rate S and chemical reaction parameter β. In contrast, an increasing Eyring-Powell fluid parameter λ increases the concentration boundary layer thickness.
- The amplitude of the skin friction coefficient increases with increasing the Hartmann number M, and the ratio of oscillation frequency of the sheet to its stretching rate S, while it is suppressed with increasing the Eyring-Powell fluid parameters λ and K.
- In the limiting case when $\lambda, K \to 0$, our results reduce to the corresponding results of Wang [22].

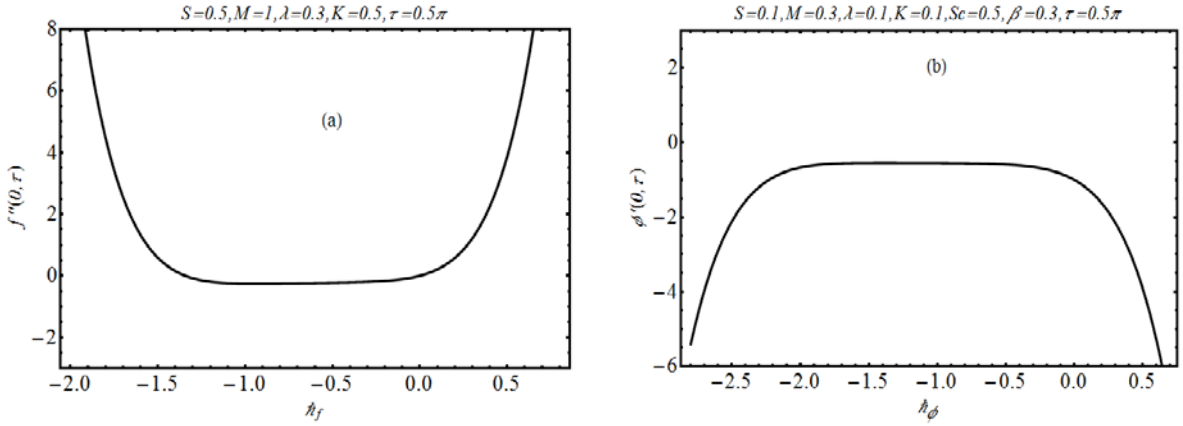

Fig. 2. The $\hbar-$ curves at 6^{th} order of approximation: (a) for velocity; (b) for concentration profile.

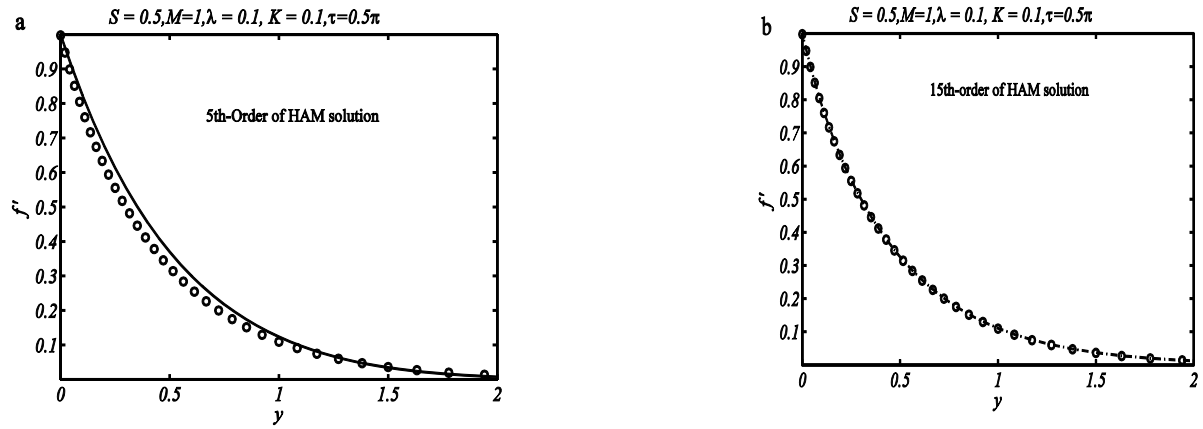

Fig. 3. Comparison of $f'(y,\tau)$ obtained from HAM solution (solid lines) and the numerical solution (open circles).

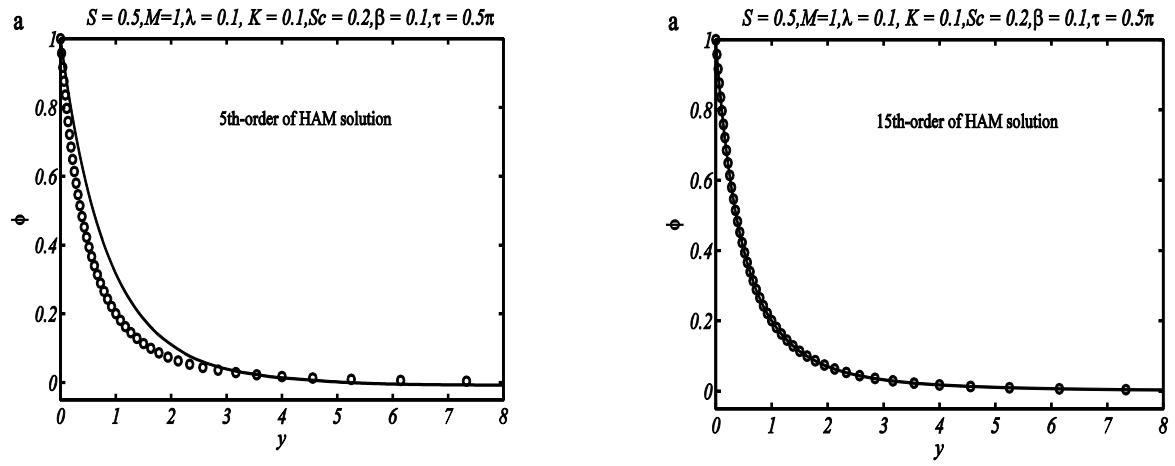

Fig. 4. Comparison of concentration field $\phi(y,\tau)$ obtained from HAM solution (solid lines) and the numerical solution (open circles).

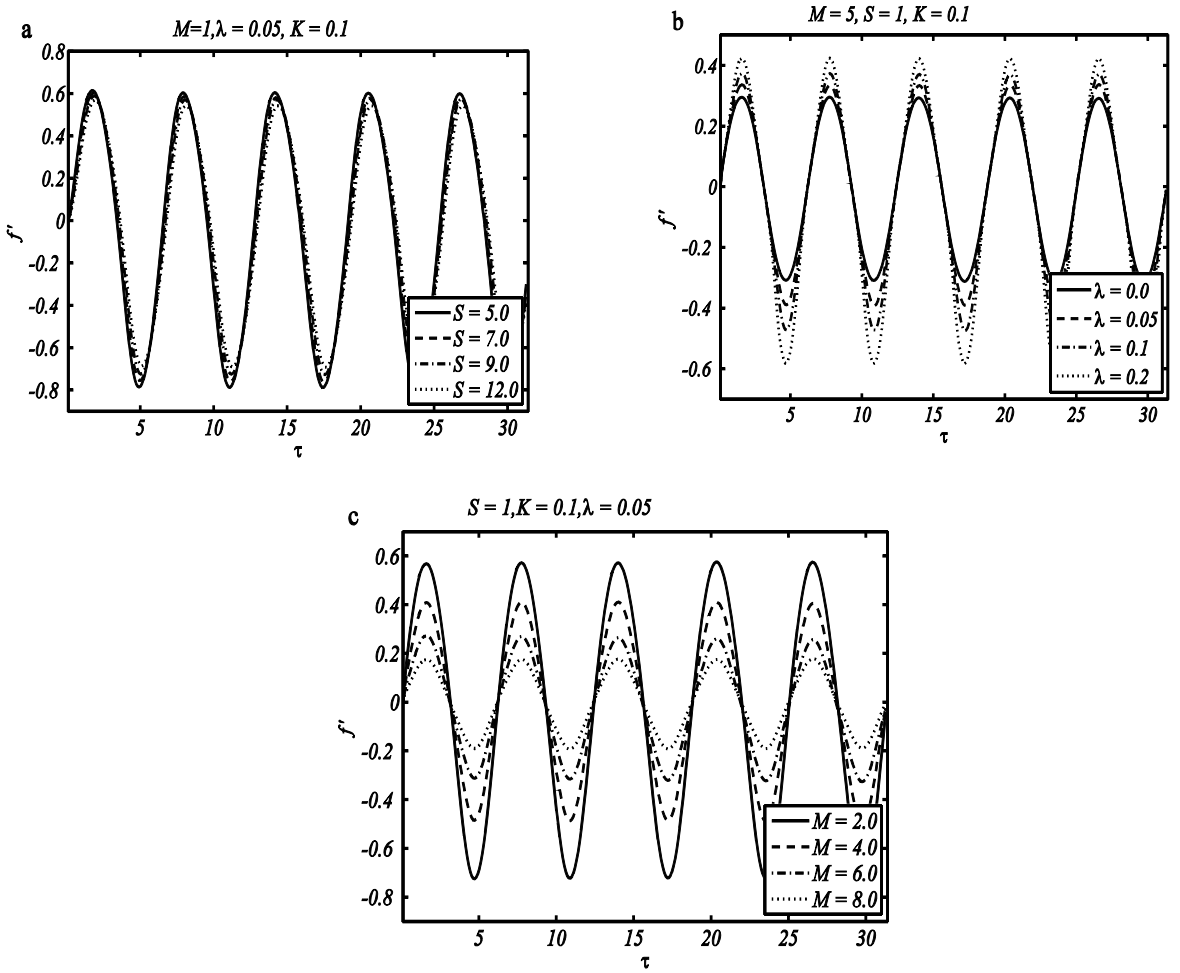

Fig. 5. Velocity profile as a function of time: (a) effects of S; (b) effects of λ; (c) effects of M.

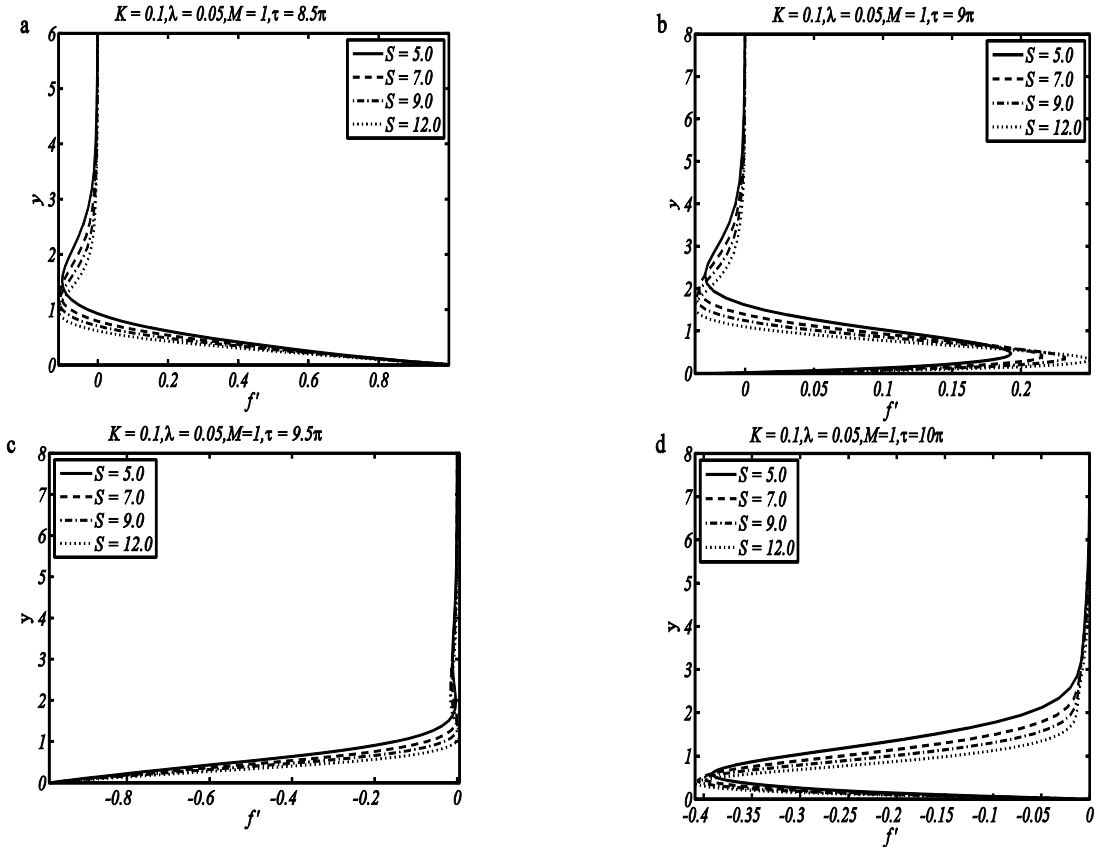

Fig. 6. Velocity field f' for different values of S.

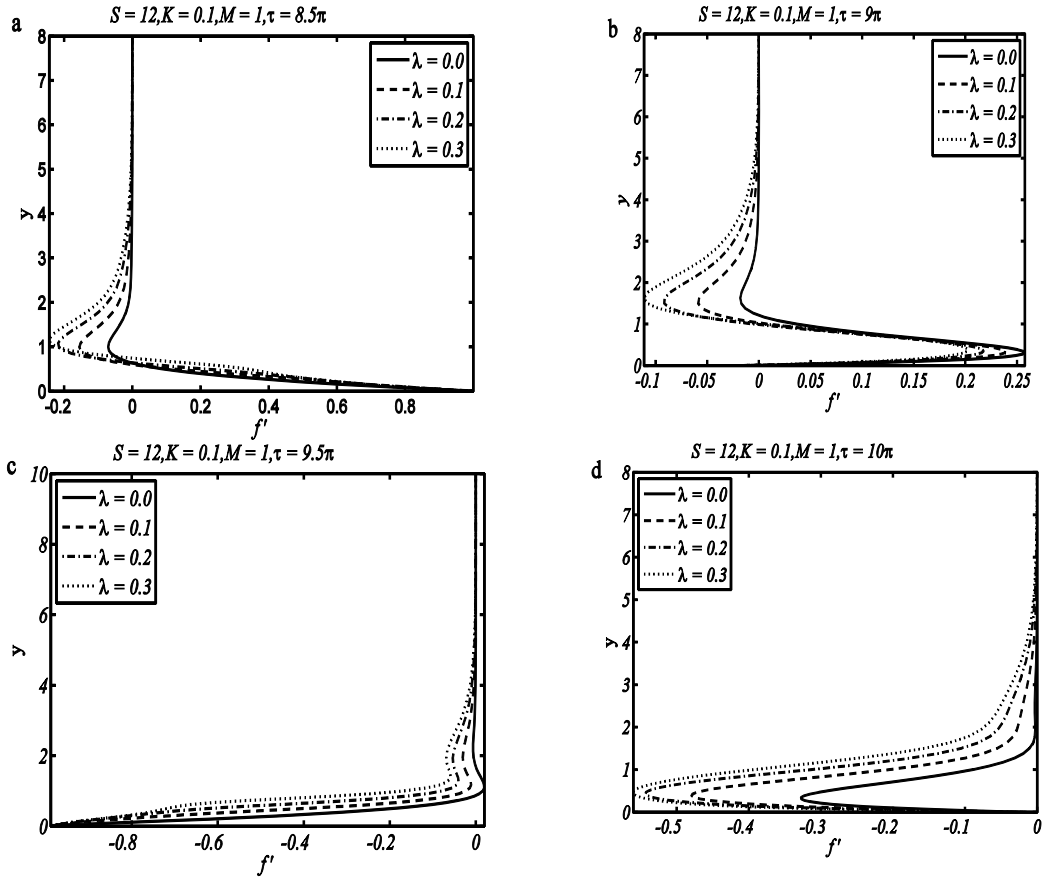

Fig. 7. Velocity field f' for different values of λ.

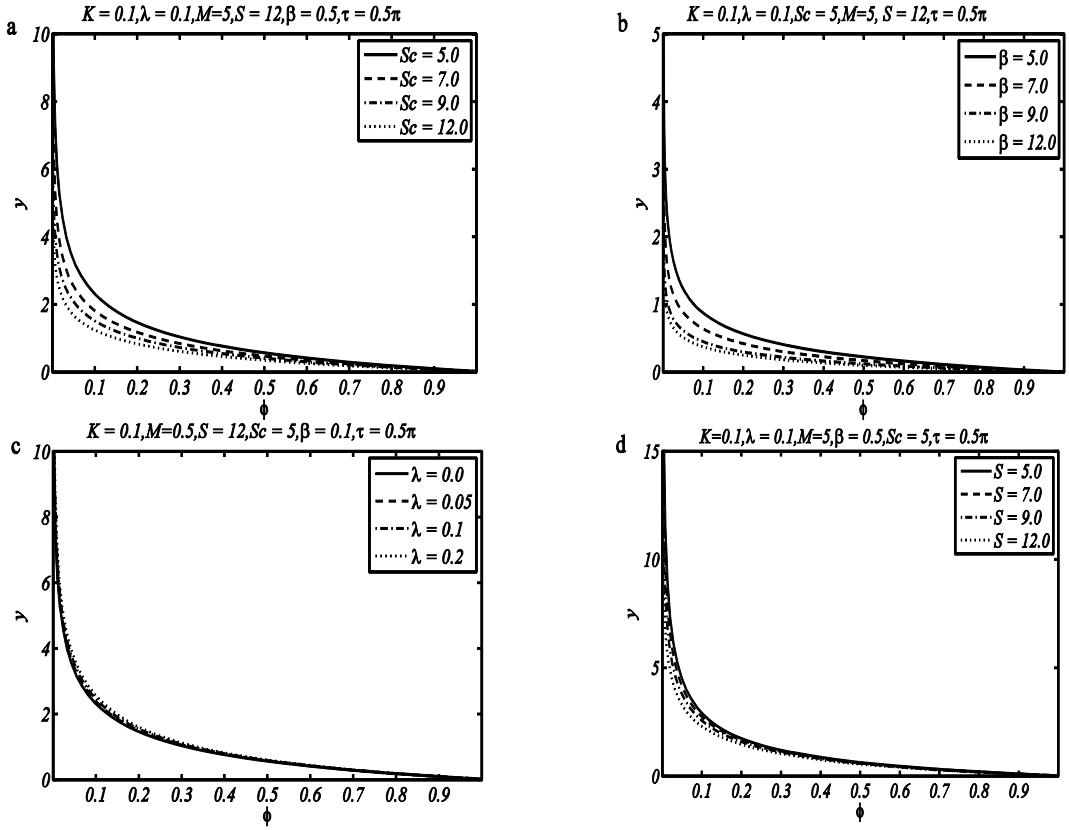

Fig. 8. Concentration field ϕ (a) effects of ; Sc (b) effects of β ; (c) effects of λ ; (d) effects of S.

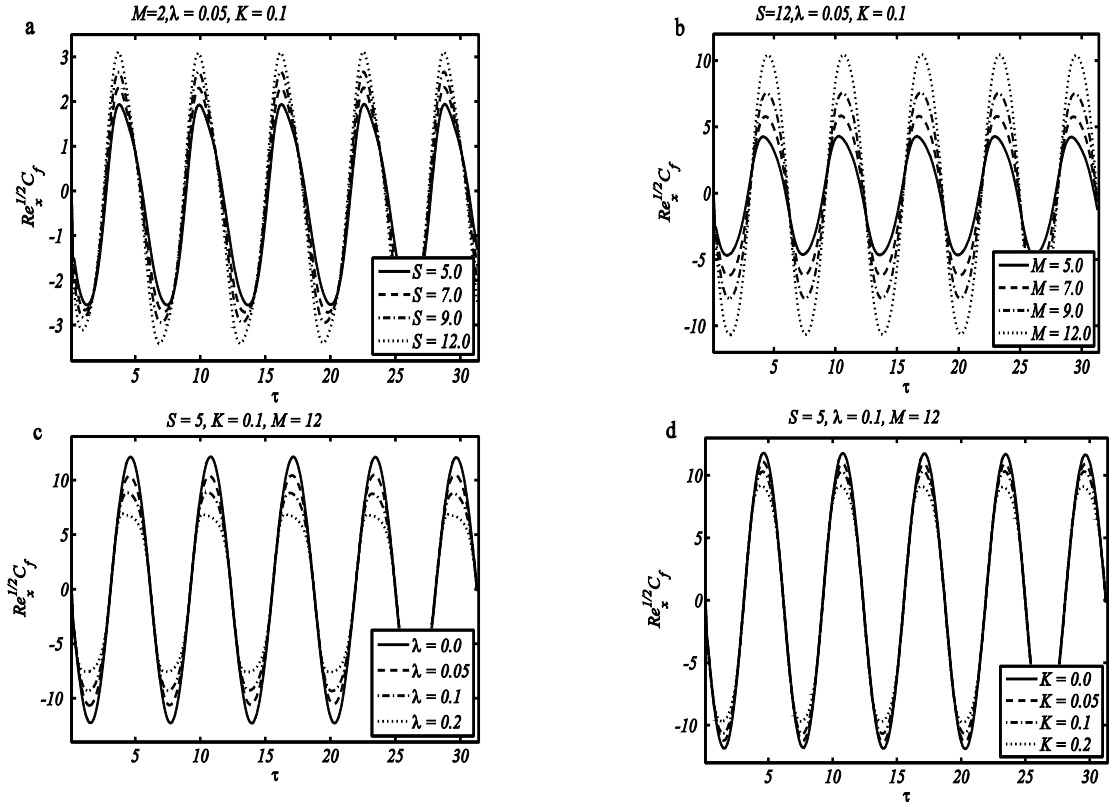

Fig. 9. The skin friction coefficient $\mathrm{Re}_x^{1/2} C_f$ as a function of time: (a) effects of S ; (b) effects of M ; (c) effects of λ ; (d) effects of K.

Acknowledegments: *We are grateful to the reviewer for his/her comments. The first author is grateful to the Higher Education Commission of Pakistan for financial assistance.*

REFERENCES

1. P. L. Chambre, J. D. Young *J, Phys. Fluids*, **1**, 48 (1958).
2. H. I. Andersson, O. R. Hansen, B. Holmedal, *Int. J. Heat Mass Tran*., **37**, 659 (1994).
3. H.S. Takhar, A.J. Chamkha, G. Nath, *Int. J. Eng. Sci*., **38**, 1303 (2000).
4. F.T. Akyildiz, H. Bellout, K. Vajravelu, *J. Math. Anal. Appl*. 320, 322 (2006).
5. T. Hayat and Z. Abbas, *Z. angew. Math. Phys.*, **59,** 124 (2008).
6. T. Hayat, M. Awais, M. Sajid, *Int J. Mod. Phys. B*, **25**(21) 2863 (2011).
7. M. A. Seddeek, A. A. Darwish, M. S. Abdelmeguid, *Comm. Nonlinear Sci. Num. Simulation*, **12**, 213(2007).
8. M.A. El-Aziz, *Chem. Eng. Commun*., **197**, 1261, (2010).
9. M. Ferdows, M. Qasem, , *Am. J. Fluid Dynamics*, **2**(6), 89, (2012).
10. K. Bhattacharyya, *Chem. Eng. Bulletin*., **15**, 6, (2011).
11. S. Mukhopadhyay, K. Bhattacharyya, *J. Egyp. Math. Society*, **20**, 229 (2012).
12. Z. Abbas, B. Ahmad, S. Ali, *J. Appl. Mech. Tech. Physics*, **56**(5), *878 (2015).*
13. T. Hayat, M. Mustafa, S. Asghar, *Nonlinear Analysis: Real World Applications*, **11**(4), 3186 (2010).
14. Z. Ziabakhsh, G. Domairry, H. Bararnia, H. Babazadeh, *J. Taiwan Inst. Chem. Engineers*, **41**, 22 (2010).
15. S. A. Kechil, *J. Porous Media*, **12**(1), 1053 (2009).
16. T. Hayat, M. Awais, Ambreen Safdar, Awatif A. Hendi, *Nonlinear Analysis: Modelling and Control*, **17** (1), 47 (2012).
17. S. A. Shehzad, T. Hayat, M. Qasim, S. Asghar, *Braz. J. Chem. Eng*., **30,** 187 (2013).
18. V. Sirohi, M. G. Timol, N.L. Kalathia, *Reg. J. Energy Heat Mass Transfer*, **6**, 219 (1984).
19. T. Javed, N. Ali,Z. Abbas, M. Sajid, *Chem. Eng. Commun*., **200**, 327 (2012).
20. T. Hayat , Z. Iqbal, M. Qasim, S. Obaidat, *Int. J. Heat Mass Tran*., **55**, 1817 (2012).
21. T. Hayat, S. Asad, M. Mustafa, A. Alsaedi, *Plos One*, **9**(7), e103214 (2014)..
22. C. Y. Wang, *Acta Mech*.. **72,** 261 (1988).
23. B. Siddappa, S. Abel, V. Hongunti., *ll Nuovo Cimento* D, **17**, 53 (1995).
24. Z. Abbas, Y. Wang, T. Hayat, M. Oberlack, *Int. J. Nonlinear Mech*., **43**,783 (2008).
25. Z. Abbas, Y. Wang , T. Hayat, M. Oberlack *Int. J. Numer. Meth*. Fl., **59**, 443 (2009).
26. L.C. Zheng, X.Jin, X. X. Zhang and J. H. Zhang, *Acta Mech. Sinica*, **29**(5), 667 (2013).
27. N. Ali, S. U. Khan, Z. Abbas, *Z. Naturforsch*., **70**(7)a, 567 (2015).
28. S. J. Liao, *J. Ship Res*. **36**, 30 (1992).
29. S. J. Liao, *Commun. Non-linear Sci. Numer. Simulation*, **11**, 326 (2006).
30. S. J. Liao, *Int. J. Non-Linear Mechanics*, **34**(4), 759 (1999).
31. S. J. Liao, *J. Fluid Mech*., **488,** 189 (2003).
32. M. Turkyilmazoglu, *Int. J. Thermal Sciences*, **50**(5), 831 (2011).
33. M. Turkyilmazoglu, *Math. Comp. Modelling*, **53,** 1929 (2011).
34. S. Abbasbandy, A. Shirzadi, *Stud. Nonlinear Sci.*, **1**(4), 127 (2010).

АНАЛИТИЧНО И ЧИСЛЕНО ИЗСЛЕДВАНЕ НА ДИФУЗИЯТА НА ХИМИЧЕСКИ АКТИВНИ ВЕЩЕСТВА ВЪВ ФЛУИД НА EYRING-POWELL НАД НАДЛЪЖНО ОСЦИЛИРАЩА ПОВЪРХНОСТ

С.У. Хан[1*], Н. Али[2], Т. Хаят[3,4]

[1]Департамент по математика, Институт по информационни технологии COMSATS, Сахиуал, Пакистан
[2]Департамент по математика и статистика, Международен ислямски университет, Исламабад, Пакистан
[3]Департамент по математика, Университет Куаид-и-Азам, Исламабад, Пакистан
[4]Изследователска група по нелинеен анализ и приложна математика, Департамент по математика, Научен факултет, Университет „Крал Абдулазиз“ Джеда, Саудитска Арабия

Постъпила на 3 октомври, 2015 г.; коригирана на 14 юли, 2016 г.

(Резюме)

Това изследване засяга нестационарния поток на флуид на Eyring-Powell породен от надлъжно осцилираща повърхност в присъствие на химична реакция. Еластичният лист се разтяга периодично напред-назад в собствената си равнина. Изведени са уравненията на движението прилагайки основните закони за запазване на масата, на количеството движение и на дифузията. Намалени са независимите променливи чрез въвеждането на безизмерни променливи, а уравненията се решават по два метода: хомотопен анализ и неявна диференчна схема. Сравнението на резултатите по двата метода показва отлично съгласие. Физичните променливи (надлъжната скорост и масовата концентрация са подробно изследвани за различни параметри.